Publications of the Korean Astronomical Society
**30**: 179 ∼ 182, 2015 September

pISSN: 1225-1534
eISSN: 2287-6936
http://dx.doi.org/10.5303/PKAS.2015.30.2.179

# SIMULATED IMPACTS TO NON-MAGNETIC CATACLYSMIC VARIABLE DISKS

M. M. Montgomery, N. Howell, and C. Schwarz
University of Central Florida, Physics Department, 4000 Central Florida Boulevard, Orlando, FL 32816, USA
*E-mail: Michele.M.Montgomery@ucf.edu*
*(Received November 30, 2014; Reviced May 31, 2015; Aaccepted June 30, 2015)*

## ABSTRACT

Dust has recently been found to be prevalent in compact binaries such as non-magnetic Cataclysmic Variable systems. As a possible source of this dust is from solid bodies, we explore impacts to non-magnetic Cataclysmic Variable disks. We use three-dimensional Smoothed Particle Hydrodynamic simulations to search for impact signatures. From injections of whole bodies to these disks, we find pulse shapes in simulated bolometric light curves that resemble impact flashes in the light curves of the Shoemaker-Levy 9 event. As a result, we tentatively identify these light curve shapes as signatures of impacts.

*Key words:* binaries: close - dust, extinction - Infrared: stars - novae, cataclysmic variables - Stars: dwarf novae

## 1. INTRODUCTION

Infrared excesses are largely attributed to dust being present in a variety of celestial systems, such as in the largest ring of the planet Saturn, in disks around isolated white dwarfs [e.g., Zuckerman & Becklin (1987), Koester et al. (1997), Kuchner et al. (1998)], and in disks of close binary systems such as Cataclysmic Variables (CVs) [e.g., Howell et al. (2006), Brinkworth et al. (2007), Hoard et al. (2007), Howell et al. (2008), Hoard et al. (2009)]. More than sixty dusty white dwarfs have been found, mostly due to the WIRED Survey(Debes et al., 2011).

For an isolated white dwarf, an infrared excess over the photosphere suggests a dust disk or dust/gas disk surrounding the compact object. In these systems, no significant luminosity is seen from an accretion disk, implying a gas accretion disk is not present. As the dust thickness is on the order of the size of dust grains (i.e., around ten microns), the dusty disk is thought to be geometrically thin. Because the gravitational settling times of metals in hydrogen-rich (DA) white dwarf atmospheres are short (i.e., from a few days up to 1000 years), the metals must be continuously re-supplied by one or more sources. The most likely source is the tidal disruption of a comet or an asteroid [see Jura et al. (2003)], with the latter being cited more [see e.g., Reach et al. (2005), Zuckerman et al. (2007), Farihi (2011), and Zuckerman et al. (2011)]. The asteroid is thought to have been perturbed by a orbiting exoplanet remnant. Of the asteroid types, processed asteroids are the type found so far to be the polluters of white dwarf atmospheres [see Farihi (2011)and Zuckerman et al. (2011)]. The processed asteroid could be from either the lithosphere of a differentiated terrestrial, possibly water-rich, first-generation exoplanet [see Farihi (2011)and Zuckerman et al. (2011)] or from a differentiated, terrestrial, possibly water-rich, second-generation exoplanet that formed from a disk of recycled, post-main sequence evolutionary material.

In nearly all CVs observed with *Spitzer*, an infrared excess is observed, and the excess is attributed to thermal emission from dust larger than ten microns [see Hoard (2012)]. Sometimes the dust is found around the CV system in a circumbinary dust disk (see Figure 1). An example is V592 Cas [see Hoard et al. (2009)]. However, sometimes the dust is found within the white dwarf's Roche lobe but outside the gas accretion disk (see Figure 2). Examples are WZ Sge. Z Cha, and SS Cyg [see Howell et al. (2008) and Gaudenzi et al. (2011)]. For the former, the dust disk is assumed to start at the tidal truncation radius, which is outside the CV. For the latter, the dust disk is assumed to start at the dust sublimation temperature.

The dust disks around isolated white dwarfs and in both the circumbinary and the circumstellar non-magnetic CV systems contain about the same mass of dust [see e.g., Hoard et al. (2009). This mass is about that of a medium-to-large asteroid in the Solar System (i.e., $\sim 10^{21}$-$10^{23}$ g).

Sources for the dust in a CV circumbinary dust disk could be from dust generated in an ejected common envelope, dust lost from the accretion flow, dust and gas lost from the inner Lagrange point [see e.g., Bisikalo et al. (1998) and Bisikalo & Kononov (2010)], dust produced in the outer atmosphere of the donor star that was transported from the binary by mass outflows during nova or outbursts [see e.g., Ciardi et al. (2006), and/or dust transported by a wind from the disk and/or the

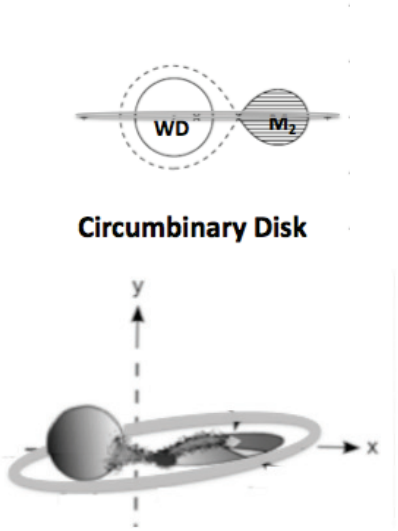


Figure 1. Cartoon of an edge-on (left panel) and a tilted (right panel) circumbinary dust disk (gray ring) around a non-magnetic CV system, which consists of a white dwarf (WD) in a close binary with a secondary mass star ($M_2$).


Figure 2. Cartoon of a dust disk (gray ring) surrounding the gas disk around a white dwarf in a non-magnetic CV system.

white dwarf.

Sources for the dust in the ring around the gas disk in a non-magnetic CV system could be from dust grains that formed in the outer atmospheres of donor stars and transported through the inner Lagrange point. Another possible source is a tidally disrupted comet or asteroid [see Hoard (2012)]. As the grain sizes are larger than ten microns (and likely even significantly larger as smaller grains are removed by radiation pressure and sublimation) and the mass content is about that of a medium-to-large asteroid, the latter source becomes more probable than possible. As such, in this work we consider the latter source.

In this work, we use three dimensional Smoothed Particle Hydrodynamic (SPH) simulations to generate a gaseous non-magnetic CV accretion disk. We inject an asteroid-sized body into the accretion disk from a point just inside the Roche lobe of the white dwarf. We search for signatures in the light curve and the accretion disk that indicate an impact to the CV system has occurred. In §2, we introduce the 3D SPH code and model parameters. In §3, we present our results and discuss them. We conclude and discuss future work in §4.

Table 1
Input Parameters

| Parameter | Value |
|---|---|
| White Dwarf Mass $M_1$ | 0.6 $M_\odot$ |
| Secondary Star Mass $M_2$ | 0.27 $M_\odot$ |
| q=$M_2/M_1$ | 0.45 |
| Orbital Period $P_{orb}$ | 2.86 hours |
| Orbital Separation $a$ | 0.97 $R_\odot$ |
| alpha viscosity parameter | 0.5 |
| beta viscosity parameter | 0.5 |
| Smoothing length | 0.02 |
| Number of Particles | 25,000 |

## 2. THE SPH CODE AND INPUT PARAMETERS

In this work, we use the 3D SPH codes used and described in e.g., Montgomery (2009) that has its roots in Simpson (1995). The root code [i.e., Simpson (1995)] has been designed to simulate accretion disks in non-magnetic CV systems. It uses the Lagrangian method of SPH, has a maximum of 25,000 particles, assumes an ideal gas law with a low adiabatic gamma, and does not include radiation effects or magnetic fields. The only unknown is alpha in the Shakura & Sunyaev (1973) alpha-disk model. In all simulations, the primary and secondary stars are treated as point masses, and gas particles are injected through the inner Lagrange point $L_1$ to build the disk.

In this work, an accretion disk is built from scratch by injecting ten particles per time step through the inner Lagrange point until an accretion disk of 25,000 particles has formed. Table 1 lists the input parameters.

The simulation is run for several thousand orbits, during which time the disk tilts out of the orbital plane as discussed in e.g., Montgomery (2012). Several orbits later, the disk returns to the orbital plane and the cycle repeats one or more times. We do not discuss this result in this work and save the result for a future publication as it is not the subject of this work.

At orbit 2000, the simulation is stopped and three asteroid-like bodies are artificially introduced just inside the white dwarfs Roche lobe, near the inner Lagrange point. In this work, we neither speculate how bodies of this size and mass are formed nor why they are located at this point. We restart the simulation, which runs through to orbit 2050.

## 3. RESULTS AND DISCUSSIONS

Almost immediately upon injection, one of the three asteroid-like bodies is ejected from the system. The other two gravitationally fall toward the accretion disk.

Figure 3 shows snapshots of the simulated non-magnetic CV system and the impacts from the two asteroid-like bodies. As shown, the first asteroid-like body (black circle) passes over the disk in the first two snapshots before finally entering the disk at the rim in the third snapshot. The second asteroid-like body (black square) embeds itself within the disk as shown starting with the first snapshot. Note the holes gener-

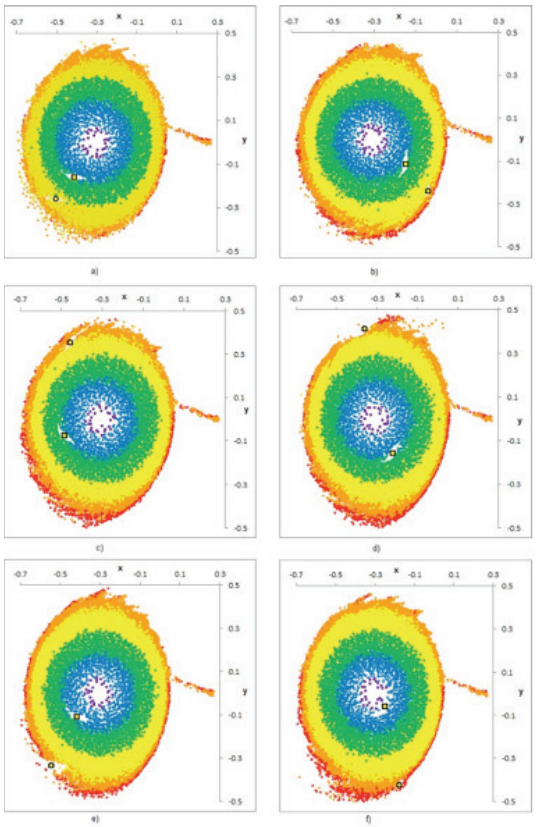

Figure 3. Snapshots of a simulated, geometrically thin, accretion disk in a non-magnetic CV system showing impacts from asteroid-like bodies. The first impacting body is the black circle and the second impacting body is the black square. Letters a) through f) represent orbits 2001, 2004, 2007, 2011, 2015, and 2019, respectively. Coolest regions of the disk are colored red whereas hottest regions are colored violet.

ated in the disk around the asteroid-like bodies, which stretch and relax as they (i.e., the holes that surround the asteroid-like bodies) orbit in the elliptical disk. Because the disk only contains 25,000 particles, the disk is geometrically thin. If the disk contained more particles, the asteroid-like body would not likely pass through the disk creating the hole, and instead may break-up into smaller bodies. Because the code is designed to only consider gas in the accretion disk, the asteroid-like body does not break into smaller pieces as it spirals down into warmer parts of the accretion disk. As such, these results are not entirely realistic. However, we are mostly interested in the impacts to the disk and any effects seen in the artificial light curves.

Figure 4 shows the artificial bolometric light curve. Two pulse shapes appear between orbits 2000 and 2001 and a third pulse shape appears between orbits 2019 and 2020. The first two pulses in the artificial light curve are due to the impacts from the asteroid-like bodies. The first impact has less of an effect on the disk as it plunges through the disk whereas the second impact embeds itself immediately upon impact. We find that amplitude of the signal is due to the amount of interaction between the asteroid-like body and the disk. The last pulse shape

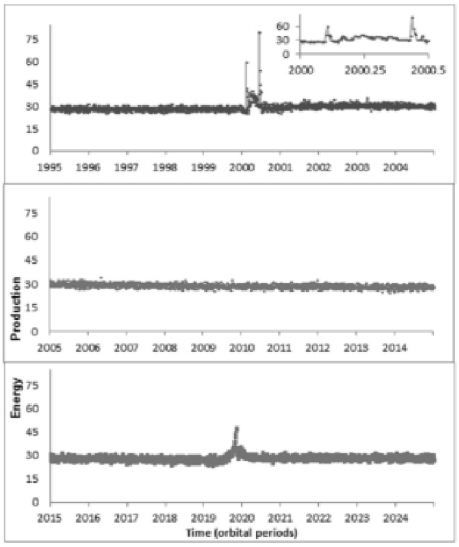


Figure 4. Artificial bolometric light curve showing pulse shapes between orbits 2000 and 2001 and again between orbits 2019 and 2020. The inset shows two of the pulse shapes in more detail.

in the artificial light curve is due to one of the asteroid-like bodies falling from the inner accretion disk into the white dwarf. The pulse shape is not from the interaction of the asteroid-like body with the atmosphere of the white dwarf but is instead from the disk readjusting to the lack of a larger body within it. The last pulse shape is likely not realistic as the asteroid-like body should have disintegrated more as it spiraled toward the white dwarf. As shown in the inset of Figure 4, the first two pulse shapes from the impacts, however, resemble pulse shapes of flash impacts by e.g., comet Shoemaker-Levy 9 to Jupiter's atmosphere [see e.g., Harrington (2004) and Sasaki et al. (1995)]. As such, we tentatively identify these pulse shapes as signatures of impacts.

From comparisons of Figures 3 and 4, we find that a large hole in the disk has no effect on the bolometric light curve. If non-magnetic CV disks had holes in them, we would not see signatures in the light curves. Nonetheless, holes in these disks seem unlikely. Another comparison is that if an otherwise gaseous disk contains large asteroid-sized bodies it is also not apparent in the light curve. If non-magnetic CV disks had large asteroid sized bodies, we would not see signatures in the light curves.

As shown in Figure 4, pulse shapes from impacts are non-cyclic and are thus are likely rare events for observation. Nonetheless, a pulse shape signature in artificial light curves may be of value should one be seen in observational light curves.

As plumes are seen in the light curves of the comet Shoemaker-Levy 9 event, plumes might also be seen in

light curves of non-magnetic CV systems. The plumes occur after the impacts and after the fireball of material rises in altitude. Plumes are the raining of the gaseous material back down to the planet. Not seeing plumes in our artificial light curves of non-magnetic CV disks is likely due to poor resolution from using 25,000 particles. As plume signatures in light curves have higher amplitudes and last significantly longer than impact signatures, simulations with higher resolution to generate plumes signatures may be of value and is left for future work.

## 4. CONCLUSIONS

In this work, we inject asteroid-sized objects into non-magnetic CV accretion disks to search for signatures in the artificially generated bolometric light curves. We find pulse shapes from impacts that resemble impact flashes by comets like the Shoemaker-Levy 9 event. As such, we tentatively identify these light curve shapes as signatures of impacts and confirmation is left for future work.

## ACKNOWLEDGMENTS

We are grateful to APRIM for their financial support to attend this conference and to present this work. The first author would like to thank the second author, who has since graduated with a Bachelor of Science in Physics from The University of Central Florida. The first author would like to thank the third author, who has since graduated as is now a post-doc at The University of Central Florida in the Chemistry and CREOL Departments. We would also like to acknowledge the NSF Young Entrepreneur and Scholar program at UCF through which this directed undergraduate research work was made possible.

## REFERENCES

Bisikalo, D. V., Boyarchuk, A. A., & Chechetkin, V. M., et al., 1998, Three-dimensional Numerical Simulations of Gaseous Flow Structure in Semidetatched Binaries, MNRAS, 300, 39

Bisikalo, D. V. & Kononov, D. A., 2010, Mass Exchange in Close Binaries: Theories VS Observations, MmSAI, 81, 187

Brinkworth, C. S., Hoard, D. W., & Howell, S. B., et al., 2007, Spitzer Space Telescope Observations of Magnetic Cataclysmic Variables: Possibilities for the Presence of Dust in Polars, ApJ, 659, 1541

Ciardi, D. R., Wachter, S., & Hoard, D. W., et al., 2006, Spitzer Space Telescope Observations of Var Her 04: Possible Detection of Dust Formation in a Superoutbursting Tremendous Outburst Amplitude Dwarf Nova, AJ, 132, 1989

Debes, J. H., Hoard, D. W., & Wachter, S., et al., 2011, The WIRED Survey. II. Infrared Excesses in the SDSS DR7 White Dwarf Catalog, ApJS, 197, 38

Farihi, J., 2011, In White Dwarf Atmospehres and Circumstellar Environments, ed. D.W. Hoard (Wiley: Berlin), 117-171

Gaudenzi, S., Giovannelli, F., & Mandalari, M., et al., 2011, An Intrinsic Source of Reddening in the Cataclysmic Variable SS Cygni, A&A, 525, 147

Harrington, J., de Pater, I., & Brecht, S. H., et al., 2004, Lessons from Shoemker-Levy 9 about Jupiter and Planetary Impacts, in: Jupiter. The Planet, Satellites and Magnetosphere. Edited by Fran Bagenal, Timothy E. Dowling, William B. McKinnon. Cambridge Planetary Science, Vol. 1, Cambridge, UK: Cambridge University Press, p. 159-184

Hoard, D. W., 2012, Dust in White Dwarfs and Cataclysmic Variables (An Observational Perspective), MmSAI, 83, 490

Hoard, D. W., Howell, S. B., & Brinkworth, C. S., et al., 2007, The Mid-Infrared Spectrum of hte Short Orbital Period Polar EF Eridani from the Spitzer Space Telescope, ApJ, 671, 734

Hoard, D. W., Kafka, S., Wachter, S., et al., 2009, Observations of V592 Cassiopeiae with the Spitzer Space Telescope - Dust in the Mid-Infrared, ApJ, 693, 236

Howell, S. B., Brinkworth, C, & Hoard, D. W., et al., 2006, Spitzer Space Telescope Observations of Magnetic Cataclysmic Variables: Evidence of Excess Emission at 3-8 $\mu$m, ApJ, 646, L65

Howell, S. B., Hoard, D. W., & Brinkworth, C., et al., 2008, 'Dark Matter' in Accretion Disks, ApJ, 685, 418

Jura, M., Farihi, J., & Zuckerman, B., et al., 2007, Infrared Emission from the Dusty Disk Orbiting GD 362, an Externally Polluted White Dwarf, AJ, 133, 1927

Koester, D., Provencal, J., & Shipman, H. L., 1997, Metals in the Variable DA G29-38, A&A, 320, L57

Kuchner, M. J., Koresko, C. D. & Brown, M. E. 1998, Keck Speckle Imaging of the White Dwarf G29-38: No Brown Dwarf Companion Detected, ApJ, 508, L81

Montgomery, M. M., 2009, Atlas of Tilted Accretion Disks and Source to Negative Superhumps, MNRAS, 394, 1897

Montgomery, M. M., 2012, Numerical Simulations of Naturally Titled, Retrogradely Precessing, Nodal Superhumping Accretion Disks, ApJ, 745, L25

Reach, W. T., Kuchner, M. J., & von Hippel, T., et al., 2005, The Dust Cloud Around the White Dwarf G29-38, ApJ, 635, L161

Sasaki, S., Yabe, T., & Abe, Y., et al., 1995, Explanation of IR-Light Curves of Shoemaker-Levy 9 Impacts: Comparison Between Numerical Simulations and Observations, ESOC, 52, 293

Shakura, S. & Sunyaev, R. A., 1973, Black Holes in Binary Systems. Observational appearance, A&A, 149, 135

Simpson, J. C., 1995, Numerical Simulations for Three-Dimensional Smoothed Particle Hydrodynamic Simulations: Applications to Accretion Disks, ApJ, 448, 822

Zuckerman, B. & Becklin, E. E., 1987, Excess Infrared Radiation from a White Dwarf - an Orbiting Brown Dwarf?, Nature, 330, 138

Zuckerman, B., Koester, D., & Dufour, P., et al., 2011, An Aluminum/Calcium-rich,Iron-poor, White Dwarf Star: Evidence for an Extrasolar Planetary Lithosphere? ApJ, 739, 101

Zuckerman, B., Koester, D., & Melis, C., et al., 2007, The Chemical Compositon of an Extrasolar Minor Planet, ApJ, 671, 872